Al-Rafidain Engineering Journal (AREJ) Vol.31, No.1, March 2026, pp. 94-102

Confocal Microwave Imaging for Brain Diagnostics: A Performance Assessment of DAS and MVDR Beamforming Algorithms using Realistic Head Models

☒**Rahmah J. Abdulkareem**
rahmah.abdulkareem@uoninevah.edu.iq

Younis M. Abbosh
younis.abbosh@uoninevah.edu.iq

Dia M. Ali
dia.ali@uoninevah.edu.iq

Biomedical Engineering, Electronics Engineering, Ninevah University, Mosul, Iraq

Received: Aug 9th, 2025 Received in revised form: Aug 28th, 2025 Accepted: September 3th, 2025

ABSTRACT

Confocal Microwave Imaging (CMI) has recently emerged as a promising non-invasive method for detecting brain tumors, leveraging the dielectric difference between healthy and diseased tissues. This study evaluates the effectiveness of two leading beamforming algorithms—Delay and Sum (DAS) and Minimum Variance Distortionless Response (MVDR)—for confocal image reconstruction using simulated S-parameter data from CST Studio Suite v2024. Various head models were used, including homogeneous, symmetric heterogeneous, and realistically detailed heterogeneous (HUGO voxel) models. Both single- and multiple-tumor scenarios were explored. The MVDR algorithm significantly outperformed DAS in terms of tumor localization and spatial resolution, particularly in complex models and deep tissue layers, as demonstrated in our simulations. Adaptive beamforming techniques also achieved better spatial accuracy and contrast in heterogeneous brain phantoms. These results highlight the diagnostic potential of MVDR-based CMI systems and lay the groundwork for future advancements through the use of larger antenna arrays and the integration of machine learning strategies to enhance imaging performance.

Keywords:

Confocal Microwave Imaging; Brain Tumor Detection; Delay and Sum (DAS); Minimum Variance Distortionless Response (MVDR).

https://jamh.uomosul.edu.iq/index.php/rengj
Email: alrafidain_engjournal3@uomosul.edu.iq

1. INTRODUCTION

Recently, Confocal Microwave Imaging (CMI) has been rapidly proposed as a promising non-invasive technique for detecting tumors at early stages. In this context, this study explores the application of CMI in medical imaging for brain diagnostics and treatment, providing high-contrast dielectric maps that identify abnormal regions associated with tumors. Arrays of circular patch antennas and the DAS beamforming algorithm are intrusive for an electronic system, which synthetically focuses microwaves to visualize the internal structures of the human brain [1]. Therefore, CMI has been considered a potential imaging method for the brain due to its several advantages, including safety (non-ionizing radiation), the ability to move the system around without incurring significant costs, and the remarkable contrast between the dielectric properties of normal and abnormal tissues. As an alternative to costly and not always readily available MRI or CT methods, CMI holds promise for stroke detection and tumor assessment, especially in early-stage diagnosis [2]. This study examines the practical application of these challenges in simulations and model solutions. Although CMI offers clear benefits, obstacles remain; for example, skull attenuation is a significant limitation, and clinical validation remains limited. According to the study, time-domain adaptive beamforming enhances signal focusing and noise suppression in microwave imaging [3].

Additionally, it is suggested that combining machine learning with CMI systems will improve tumor targeting and enhance image reconstruction [3]. Early detection of tumor tissue, based on the high dielectric contrast between normal and pathological tissues, demonstrates that CMI has excellent potential for early tumor diagnosis. Furthermore, the inherent nature of CMI in brain imaging shows its suitability for safe, economical, and portable brain scans. To achieve this, the method focuses microwave signals to create a 3D image of the brain's internal structure, using a circular array of microstrip patch antennas and time-domain algorithms such as DAS and MVDR [4]. Compared to traditional imaging techniques like MRI or CT, which involve ionizing radiation and are often costly or unavailable, CMI offers practical advantages: it is non-ionizing, fast, and less expensive. This method can detect dielectric anomalies related to the presence of tumors, as further demonstrated through models of the simulated brain.

2. RELATED WORK

Lim et al. (2008). – Confocal Microwave Imaging for Breast Cancer Detection: Delay Multiply and Sum Algorithm.

Proposed a DAS-based confocal imaging system enhanced by Delay Multiply and Sum (DMAS), achieving improved lesion detection and image clarity compared to conventional DAS techniques. This work formed the foundation for subsequent studies on confocal imaging in complex biological tissues [5].

Mohd Aminudin Jamlos et al. (2019). – An Improved Confocal Microwave Imaging Algorithm for Tumor Detection.

They developed an improved DAS algorithm (uDAS) using UWB antennas on a head phantom, which resulted in sharper and higher-contrast brain tumor imaging. The approach enhanced backscatter focusing, leading to more accurate tumor localization [6].

Rahmat Ullah & Tughrul Arslan (2020). – Parallel Delay Multiply and Sum Algorithm for Microwave Medical Imaging Using Spark Big Data Framework.Implemented DMAS in a parallel Spark MapReduce framework, enabling near real-time confocal image reconstruction while maintaining diagnostic accuracy. This advancement addressed computational bottlenecks, making confocal imaging more feasible for clinical applications [7].

Abbosh et al. (2023). – Synthetic Microwave Focusing Techniques for Medical Imaging: Fundamentals, Limitations, and Challenges.

The study presented a comprehensive review of various synthetic microwave focusing techniques, such as time reversal, DAS, and confocal imaging. The study highlighted that all these methods are based on simplified scalar electromagnetic scattering assumptions, which limit their accuracy in heterogeneous tissues. It highlighted current challenges, such as the oversimplification of tissue models, and proposed potential solutions, including calibration, adaptive multi-frequency approaches, dispersive modeling, and deep learning augmentation [8].

Abbosh, S., & Guo (2025). – Techniques to Enhance Performance of Confocal Algorithm in Medical Microwave Imaging. Investigated methods to enhance confocal microwave imaging by addressing challenges like clutter, limited resolution, and heterogeneity. Through full-wave simulations, the study demonstrated that clutter suppression and algorithmic optimization significantly improve signal-to-clutter ratio (SCR) and tumor localization in biomedical imaging [9].
These studies collectively highlight both the progress and challenges in confocal microwave imaging. While algorithmic improvements (DMAS, uDAS, parallel implementations) enhanced resolution and reduced noise, limitations in heterogeneous environments remain significant. The review by Abbosh et al. (2023) underscores these limitations and the need for adaptive and hybrid methods. Building on this foundation, the current work focuses on evaluating DAS and MVDR beamforming techniques in realistic brain phantoms, aiming to address some of these open challenges.

3. SIGNAL CALIBRATION IN CONFOCAL MICROWAVE BRAIN IMAGING

In CMI systems for brain diagnostics, signal calibration is a crucial preprocessing step that enhances imaging accuracy and improves tumor localization. Due to the layered and heterogeneous nature of cranial tissues—including the scalp, skull, CSF, and brain parenchyma — early-time reflections can dominate the measured signals, masking the weaker backscatter from minor anomalies such as tumors or hemorrhagic zones [10].

4. SOURCES OF UNDESIRED SIGNALS:

4.1 Monostatic Configuration:

- Antenna self-reflection due to impedance mismatch.
- Strong reflections from the scalp–air and scalp–skull boundaries.
- Initial pulse reflections are unrelated to deep targets [11].

4.2 Multistatic Configuration (used in CMI):

- Antenna-to-antenna mutual coupling, especially with closely packed array setups.

- Interface reflections between scalp, skull, CSF, and brain tissue layers.
- Variations in antenna polarisation and signal path length cause system-intrinsic clutter [12].

The late-time clutter also emerges as a result of the complex scattering at boundaries among different brain tissues (i.e., between white matter, grey matter, and abnormal tissues) in addition to early-time reflections. These are the interferences that shit all over the confocal summation process, an algorithm like DAS & MVDR relies on to make images, producing false hotspots or poorly defined reconstructions[13].

5. CALIBRATION AND CLUTTER SUPPRESSION TECHNIQUES:

To address these issues in CMI, several preprocessing and calibration techniques are applied:

- Averaging of healthy-scan responses to reduce static boundary reflections.
- Reference subtraction, where known baseline (tumor-free) datasets are removed from the measured data[14].
- Singular Value Decomposition (SVD) and Eigenvalue Filtering to remove dominant artefact modes.
- Time gating, applied before DAS beamforming, isolates only relevant late-time responses related to tumor scattering [15].

Applying these signal conditioning methods before beamforming helps CMI systems focus microwave energy at specific voxels in the brain, resulting in better detection of dielectric anomalies and a higher CNR in the reconstructed images.

6. MAIN ALGORITHMS IN MICROWAVE CONFOCAL IMAGING

CMI is an emerging and promising brain diagnostic modality, which is a passive way to detect tumors and stroke regions in the brain. Instead of recovering complete dielectric profiles, as in tomography, CMI samples the energy maps formed by backscattered signals to localize strong scatterers. Among the beamforming algorithms, the following two algorithms have been used:

- DAS: Coherent-sum method based on SAR processing for simplicity and real-time implementation [16]
- MVDR: An adaptive beamformer for improving spatial resolution and clutter suppression. [17]

7. BRAIN PHANTOM DESIGN AND SIMULATION SETUP

This section details the design and simulation setup for our Confocal Microwave Imaging (CMI) system, specifically justifying the adoption of a four-antenna model. This work builds upon established principles in microwave imaging and addresses limitations identified in previous research, aiming to enhance the accuracy and reliability of brain diagnostics.

7.1 Foundation in Previous Work and System Evolution

This approach is grounded in extensive research that demonstrates the potential of CMI for medical imaging. Early foundational studies, such as those by Hagness et al. (1998) and Guo et al. (2006) [1][4], established the groundwork for pulsed microwave confocal systems and adaptive beamforming methods using antenna arrays for cancer detection, particularly in applications like breast cancer detection.

Building on these initial developments, the core concept of employing circular arrays of microstrip patch antennas with time-domain algorithms such as Delay and Sum (DAS) and Minimum Variance Distortionless Response (MVDR) has become a consistent theme in CMI development for focusing microwave signals to create 3D images of internal brain structures.

This study specifically focuses on applying and enhancing CMI for brain diagnostics and treatment, providing high-contrast dielectric maps to identify abnormal regions associated with tumors within the brain. Previous microwave imaging simulations for the head, particularly those using heterogeneous head models, often faced limitations. For instance, combining them with heterogeneous head models "precluded more precise image reconstruction," and the resulting images "did not have an acceptable resolution or sufficiently high fidelity to detect tumors unambiguously". To overcome these challenges in brain imaging, CMI is adopted as a more robust and efficient method. CMI's ability to align backscattered signals based on time differences bypasses complex inverse reflection calculations, thereby improving image reconstruction quality and reducing simulation time, which are critical for clinical and real-time brain imaging.

7.2 Design an Antenna Model

To overcome the challenges of achieving comprehensive brain imaging, the proposed system employs four symmetrically arranged patch antennas around the human head model at 0°, 90°, 180°, and 270°, with a 10 mm gap from the head to ensure full spatial coverage and efficient transmission/reception of microwave signals as shown in Fig 1 and Fig. 2. Patch antennas were selected for this design due to their optimal performance at the target frequency of 1 GHz, compact structure, ease of integration into portable systems, and ability to achieve efficient electromagnetic coupling with brain tissues while minimizing signal reflections. The optimized antenna exhibits a return loss (S11) of –26 dB at 1 GHz, ensuring minimal power loss at the bio-tissue interface and enabling a penetration depth of ~23 cm, which is sufficient to cover the entire brain volume and detect abnormalities with high accuracy.

The antenna, designed on an FR-4 lossy substrate (εr = 4.3, tanδ = 0.025, μr = 1, thermal conductivity = 0.3 W/m · K), has dimensions of 120 × 120 mm, as shown in Table 1. These dimensions were carefully optimized in CST Studio Suite 2024 to operate efficiently in the desired band.

Simulation results confirm excellent performance with |S11| ≈ –26 dB (Fig. 3), a maximum gain of 6.24 dB, and a directive far-field radiation pattern (Fig. 4), making the design highly suitable for precision, high-resolution image reconstruction in Confocal Microwave Imaging (CMI).

The antenna structure's dimensions can be optimized for the desired frequency range and dielectric properties. This optimization process will ensure the optimal performance of the MWI system in detecting brain tumors with high accuracy.

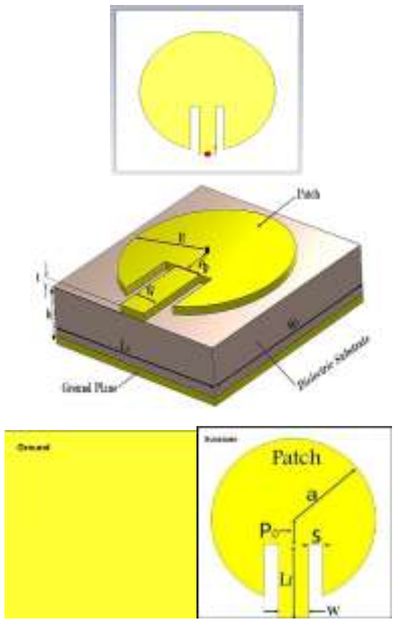

(b) (a)

Fig. 1: Patch antenna. (a) patch (top view) (b)ground plane (bottom view)

Table 1: The simulated physical dimensions of the proposed circular patch antenna for dielectric constant ϵ_r = 4.3.

parameter	Value (mm)
Radius of the patch a / R	44.5
Feeding point location ρ_o	11.8
Feed line width w	11
Feed line Length L_{50}	35
Width of Substrate w_s	120
Length of Substrate L_s	120
Width of inset cut S	5.5
patch thickness	0.035
substrate thickness	1.6

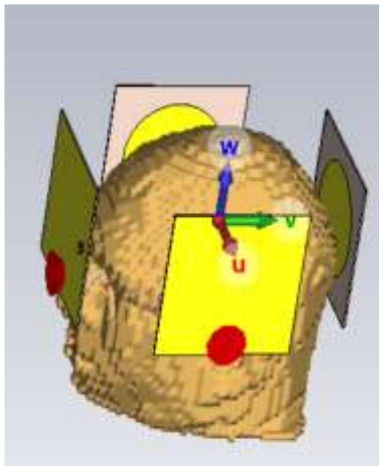

Fig. 2: Microwave Imaging system simulated in CST using patch antenna.

The dimensions were optimized to operate efficiently within the desired frequency band, typically around 1 GHz, where the antenna exhibits excellent performance with a measured S11 ≈ of 26 dB.

Fig. 3 displays the simulated |S11|, which illustrates the antenna's performance in terms of its reflection coefficient.

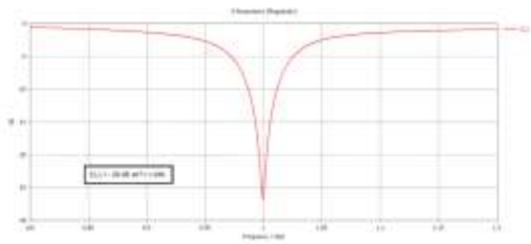

Fig. 3: |S11| of the designed Patch antenna.

Fig. 4 illustrates the directive far-field radiation pattern of the antenna, which has a maximum gain of 6.24 dB.

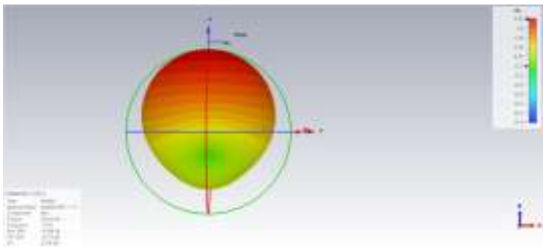

Fig. 4: Far-field radiation pattern of the patch antenna.

7.3 Brain Phantom Models for Realistic Simulation

To validate the effectiveness of our CMI system and the chosen antenna configuration, two main brain phantom hypotheses were developed using CST Studio Suite v2024 to emulate the human head for microwave imaging simulations:

- **First hypothesis: Heterogeneous Multilayer Circular Phantom:** This model consists of concentric layers representing various biological tissues—skin, fat, muscle, and bone—surrounding the brain region as shown in Fig. 5. This design simulates realistic electromagnetic responses in layered brain tissues, which is crucial for accurate simulation of microwave interaction, thereby enhancing the accuracy and reliability of CMI results.

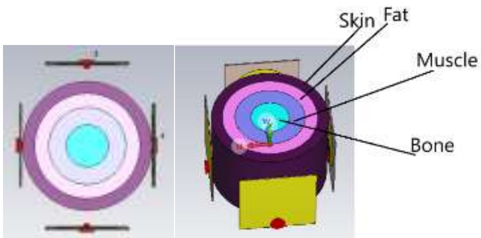

Fig. 5: Symmetrical heterogeneous brain phantom.

- **Second hypothesis: Heterogeneous Actual Human Head Model (HUGO model):** This more advanced model utilizes the predefined CST Voxel Family (HUGO model), which provides a highly realistic anatomical representation of the human head. It includes detailed layers such as skin, fat, bone, grey matter, white matter, and the cerebellum, as shown in Fig. 6, allowing for the testing of microwave imaging algorithms under near-clinical conditions. This model considers the varying dielectric properties of different tissues, which have a direct impact on microwave propagation and backscatter characteristics.

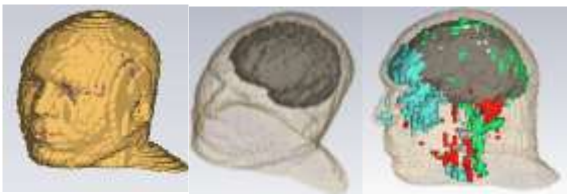

Fig. 6: Human head model using the predefined CST Voxel Family (Hugo model)

The integrated system, combining the optimised four-antenna array with these realistic brain phantoms, allows for the processing of S-parameter data using DAS and MVDR beamforming algorithms. This enables the focusing of backscattered signals at each voxel to generate reconstructed images that effectively highlight areas of high dielectric contrast, thus indicating the presence of a tumor or stroke lesion. The subsequent evaluation in Section 13 provides the empirical scientific proof of the effectiveness of this adaptation, particularly highlighting the superiority of MVDR in realistic heterogeneous models.

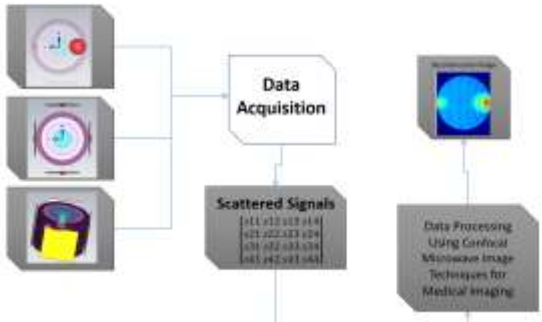

Fig. 7: Confocal Microwave Image Reconstruction Using a Symmetrical Heterogeneous Head Model - Heterogeneous brain phantom.

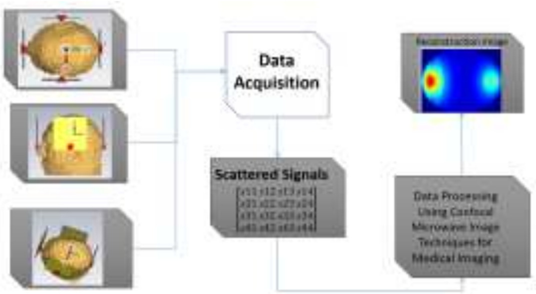

Fig. 8: Confocal Microwave Image Reconstruction Using Heterogeneous Head Model - Actual human head model using the predefined CST Voxel Family (Hugo model).

The diagram, as shown in Figs. 7 and 8 attempted to image the human brain, similar to the symmetrical Heterogeneous Head Model.

However, in this case, a realistic heterogeneous head phantom was produced using a variant from the CST Voxel Family (Hugo model), followed by a confocal imaging procedure. The different dielectric properties of several tissues, including skin, fat, bone, grey and white matter, are considered in the model. These properties have a direct effect on the microwave propagation and backscatter characteristics. Once we collect the S-parameters by applying the DAS method to them and subsequently use them to create an image, we observe a remarkable anatomical similarity of the human body based on it, as well as a perfect reproduction of pathologies, such as tumors or hemorrhagic zones.

8. IMAGE RECONSTRUCTION AND PERFORMANCE EVALUATION

In CMI, images are created by reassembling the time-reversed RF channels to obtain virtual time-reversed signals at certain positions (voxels) in the head. The (DAS) beamforming algorithm is utilised as the key appropriate algorithm in this method to temporally align the received signals according to their geometrical distances between the transducer array antennas and the point where the transmitted power is to be concentrated. When these signals are coherently summed, the energy contained in regions of high dielectric contrast (such as tumors or haemorrhages) is presensitized, and the intensity map focuses on the radiofrequency energy distribution within tissue. Additionally, an MVDR (Minimum Variance Distortionless Response) beamforming method was employed to enhance resolution and mitigate noise and side lobes. This algorithm computes adaptive weights for each signal channel to suppress signals from the opposite direction to the desired focal point, resulting in improved spatial image resolution. Beamforming was preceded by calibration of the signal using an arithmetic average procedure, which eliminated the early strong reflection caused by impedance mismatches between the antennas and bio-tissues, skin, and skull bone, respectively. This preprocessing step increased the signal-to-noise ratio (SNR) and suppressed the presence of spurious spots in the reconstructed image. Images were then examined for their potential to localize tumors, reduce noise, and detect changes in tissue conductivity. The confocal imaging approach outperformed reflectance techniques in terms of computational efficiency, image reconstruction quality, and robustness across both homogeneous and heterogeneous head models, which is consistent with previous findings reported in [18].

9. BEAMFORMING RESULTS FOR TUMOR DETECTION IN CONFOCAL MICROWAVE IMAGING

This section presents the results of brain tumor detection using Confocal Microwave Imaging (CMI), with a focus on comparing the imaging performance of two prominent beamforming algorithms: Delay-and-Sum (DAS) and Minimum Variance Distortionless Response (MVDR). These techniques reconstruct images by coherently focusing the backscattered microwave signals onto specific regions within the brain, enabling the identification of pathological areas based on dielectric contrast—particularly those indicative of tumor presence.

Reconstructed images were obtained in MATLAB by processing simulation data generated in CST Studio Suite. The simulations incorporated both realistic and simplified head phantoms, each featuring different tumor scenarios to assess algorithm robustness. Figures 9 and 11 present representative selected cases to enhance illustrative clarity.

The comparative analysis spans multiple depths and configurations to evaluate each algorithm's performance in terms of image clarity, localization accuracy, and spatial resolution. The results underscore the respective strengths and limitations of DAS and MVDR in achieving reliable electromagnetic-based tumor localization under realistic conditions.

10. IMAGE RECONSTRUCTION IN A HETEROGENEOUS HEAD PHANTOM

To further validate the effectiveness of Confocal Microwave Imaging (CMI) under practical conditions, two different heterogeneous head models were investigated. The first is a symmetric layered phantom, which provides a controlled yet realistic representation of head tissues. The second is the realistic HUGO voxel-based model, which closely mimics actual human anatomy. These two scenarios allow us to progressively evaluate the imaging algorithms, starting from structured symmetry to near-clinical complexity.

10.1 Symmetric Heterogeneous Head Phantom

To assess the performance of CMI under more realistic conditions, a symmetrically layered heterogeneous head model was employed, as illustrated in Fig. 9. The model consists of multiple concentric layers that replicate biological tissues (skin, fat, bone, and brain), with two tumors positioned at different depths and lateral locations. The symmetric radial structure enables the evaluation of the focusing capability of imaging algorithms under controlled yet heterogeneous tissue variations. Several experimental trials were conducted, yielding multiple intermediate results; however, through iterative improvements and refinements, we ultimately obtained the final reconstructed images presented in Fig. 10.

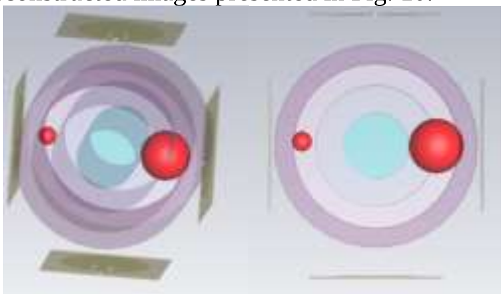

Fig. 9: Antenna-tumor configurations in CST Studio Suite for a multi-tumor scenario- Symmetric Heterogeneous Head Phantom.

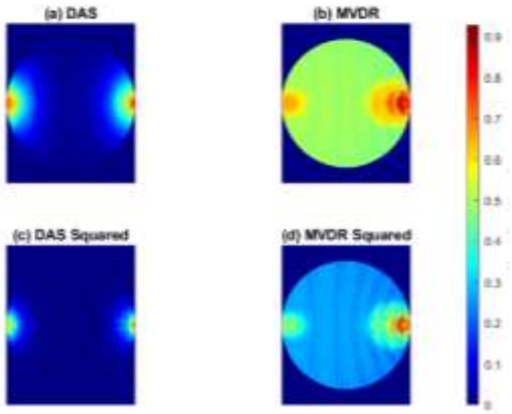

Fig. 10: Reconstructed images using beamforming algorithms in MATLAB- Symmetric Heterogeneous Head Phantom.

Fig. 9 shows the antenna–tumor arrangement in CST Studio Suite for the multi-tumor case. At the same time, Fig. 10 presents the reconstructed images obtained in MATLAB using two beamforming methods: Delay-and-Sum (DAS) and Minimum Variance Distortionless Response (MVDR). A comparative analysis of the subfigures reveals:

- DAS Image: Tumor reflections appear blurred and of low intensity near the antenna positions. The method struggles to suppress side lobes, resulting in smeared signals and poor localization.
- MVDR Image: Tumor locations are reconstructed with sharper focus and higher contrast. MVDR adaptively minimizes interference, enabling clearer separation between tumor regions and background tissues.
- DAS Squared: Contrast is slightly improved by squaring, but the tumors remain poorly localized.
- MVDR Squared (Fig. 10-d): Provides the clearest evidence of improved imaging. The tumors are sharply localized with concentrated energy, and undesired scattering is effectively suppressed. Notably, the smallest tumor, with a diameter of ≈ approximately 9 mm, was accurately detected, which demonstrates the superior spatial resolution of MVDR compared to DAS.

In summary, within this symmetric heterogeneous head model, MVDR consistently outperforms DAS primarily due to its enhanced spatial resolution and localization accuracy. The experimental proof is most evident in Fig. 10-d, where MVDR achieves clear tumor detectability and sharp boundary reconstruction. Moreover, the smallest tumor (~9 mm in diameter) is distinctly visible in MVDR, while it is blurred or nearly invisible in DAS. This result demonstrates the ability of MVDR to detect small anomalies with higher accuracy.

10.2 Realistic Heterogeneous Head Model (HUGO model)

After evaluating homogeneous and symmetric heterogeneous phantoms, they were tested on a commercially available brain-based phantom with more realistic anatomy. The realistic microwave propagation in biological head tissues was simulated by using the HUGO model of the CST Voxel Family. Featureless layers, such as skin, fat, grey matter, white matter, and the cerebellum, are included in this model, which enables the testing of microwave imaging algorithms under near-clinical conditions. Fig. 11 shows the head phantom setup for the multi-tumor case using HUGO, in which two spheres with a smaller radius were inserted into different areas inside the HUGO model. Full spatial coverage was achieved by placing antennas around the head.

Fig. 11: Antenna-tumor configuration in CST Studio Suite for multi-tumor scenario- Realistic Head Model (HUGO model)..

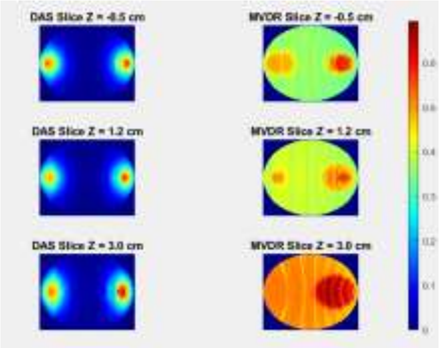

Fig. 12: Reconstructed 2D slices of brain phantom using DAS and MVDR algorithms at different depths (Z-positions) - Realistic Head Model (HUGO model).

Fig. 12 displays 2D reconstructed slices at multiple depths (Z = –0.5 cm, 1.2 cm, and 3.0 cm):

- DAS Results (left column):
  - Broad, diffused hotspots are present.
  - challenging to localize both tumors accurately due to overlapping lobes and low spatial resolution.
- MVDR Results (right column):
  - Both tumors are identified as separate, focused regions.
  - High spatial clarity enables the precise identification of tumor shape and position at all three depths.

These results further demonstrate the superiority of MVDR in handling complex anatomical environments and multiple targets.

11. EVALUATION OF RESULTS.

The non-uniform, realistic HUGO model is intricate due to electromagnetic scattering, tissue absorption, and signal distortion resulting from dielectric differences.

Nevertheless, the MVDR beamforming was consistently shown to outperform the DAS in terms of:

- High localisation accuracy.
- Sharper boundaries and better contrast.
- Robustness against both single and multiple tumor conditions.

Despite its simplicity, the DAS algorithm struggled to address the issues of blurry hotspots and interference, particularly in deeper slices or when targeting multiple areas of interference, especially on deeper slices or multiple targets.

These studies support the clinical applicability of MVDR-based confocal microwave imaging with realistic head models and tailored antenna configurations.

12. CONCLUSION

This study explored the use of Confocal Microwave Imaging (CMI) for the early detection of brain tumors, emphasizing its non-ionizing characteristics and high sensitivity to dielectric contrasts. Two beamforming algorithms—Delay-and-Sum (DAS) and Minimum Variance Distortionless Response (MVDR)—were comparatively evaluated using both simplified homogeneous phantoms and anatomically realistic heterogeneous head phantoms based on the HUGO voxel model. The proposed imaging framework was tested in multiple scenarios, including multi-tumor configurations, simplified phantoms, and voxel-based realistic head models, to comprehensively assess its performance and robustness.

Finally, based on these investigations, the main conclusions can be summarized as follows:

- The localization of brain tumors was accurate for both DAS and MVDR using the Confocal method.
- MVDR performed significantly better than DAS in terms of contrast, margin sharpness, and spatial resolution
- The proposed model can successfully reconstruct a small tumor with a minimum diameter of ≥ 9 mm.

REFERENCES

[1] S. C. Hagness, A. Taflove, and J. E. Bridges, “Two-dimensional FDTD analysis of a pulsed microwave confocal system for breast cancer detection: fixed-focus and antenna-array sensors,” IEEE Transactions on Biomedical Engineering, vol. 45, no. 12, pp. 1470–1479, Dec. 1998, doi: 10.1109/10.730440.

[2] S. Dayarathna et al., “Deep learning-based synthesis of MRI, CT, and PET: Review and analysis,” Medical Image Analysis, vol. 92, p. 103046, Jan. 2024, doi: 10.1016/j.media.2023.103046.

[3] K. An et al., “Microwave time reversal for nondestructive testing of buried minor damage in composite materials,” Inverse Problems, vol. 40, no. 4, p. 045006, Apr. 2024, doi: 10.1088/1361-6420/ad2902.

[4] B. Guo et al., “Microwave imaging via adaptive beamforming methods for breast cancer detection,” Journal of Electromagnetic Waves and Applications, vol. 20, no. 1, pp. 53–63, 2006, doi: 10.1163/156939306775777350.

[5] H. B. Lim et al., “Confocal microwave imaging for breast cancer detection: Delay-multiply-and-sum image reconstruction algorithm,” IEEE Transactions on Biomedical Engineering, vol. 55, no. 6, pp. 1697–1704, Jun. 2008, doi: 10.1109/TBME.2008.919716.

[6] M. Mozaffarzadeh, A. Mahloojifar, and M. Orooji, “Image enhancement and noise reduction using modified delay-multiply-and-sum beamformer: Application to medical photoacoustic imaging,” in Proc. Iranian Conf. on

Electrical Engineering (ICEE), 2017, doi: 10.1109/IranianCEE.2017.7985131.

[7] R. Ullah and T. Arslan, “Parallel delay multiply and sum algorithm for microwave medical imaging using Spark Big Data Framework,” Algorithms, vol. 14, no. 5, p. 157, May 2021, doi: 10.3390/a14050157.

[8] Y. M. Abbosh, K. Sultan, L. Guo, and A. Abbosh, “Synthetic Microwave Focusing Techniques for Medical Imaging: Fundamentals, Limitations, and Challenges,” Biosensors, vol. 14, no. 10, p. 498, Oct. 2024, doi: 10.3390/bios14100498.

[9] Y. M. Abbosh, K. Sultan, and L. Guo, “Techniques to Enhance Performance of Confocal Algorithm in Medical Microwave Imaging,” in Proc. 2025 Int. Multi-Conf. on Signals, Systems and Devices (SSD), 2025, doi: 10.1109/SSD64182.2025.10990004.

[10] M. E. Moudden et al., “Directivity enhancement of microstrip antennas for high-resolution brain tumor imaging using characteristic modes theory and the confocal microwave image reconstruction algorithm,” E-Prime - Advances in Electrical Engineering, Electronics and Energy, vol. 10, p. 100854, 2024, doi: 10.1016/j.prime.2024.100854.

[11] E. Ricci et al., “Performance evaluation of novel microwave imaging algorithms for stroke detection using an accurate 3D head model,” Wireless Personal Communications, vol. 96, no. 3, pp. 3317–3331, Feb. 2017, doi: 10.1007/s11277-017-4122-6.

[12] E. J. Bond et al., “Microwave imaging via space-time beamforming for early detection of breast cancer,” in Proc. IEEE Int. Conf. on Acoustics, Speech, and Signal Processing (ICASSP), 2002, doi: 10.1109/TAP.2003.815446.

[13] M. Klemm et al., “Microwave radar-based differential breast cancer imaging: Imaging in homogeneous breast phantoms and low contrast scenarios,” IEEE Transactions on Antennas and Propagation, vol. 58, no. 7, pp. 2337–2344, Jul. 2010, doi: 10.1109/TAP.2010.2048860.

[14] D. C. Lepcha et al., “Image super-resolution: A comprehensive review, recent trends, challenges and applications,” Information Fusion, vol. 91, pp. 230–260, May 2023, doi: 10.1016/j.inffus.2022.10.007.

[15] C. Yan, “A review of spectral data preprocessing techniques for machine learning and quantitative analysis,” iScience, vol. 28, no. 7, p. 112759, Jul. 2025, doi: 10.1016/j.isci.2025.112759.

[16] A. Hossain et al., “Microwave brain imaging system to detect brain tumor using metamaterial-loaded stacked antenna array,” Scientific Reports, vol. 12, p. 16478, Oct. 2022, doi: 10.1038/s41598-022-20944-8.

[17] M. A. Elahi et al., “Comparison of radar-based microwave imaging algorithms applied to experimental breast phantoms,” in Proc. XXXIInd General Assembly and Scientific Symposium of the URSI (URSI GASS), 2017, doi: 10.23919/URSIGASS.2017.8105082.

[18] S. Y. Lee, V. J. Parot, B. E. Bouma, and M. Villiger, “Confocal 3D reflectance imaging through multimode fibers without wavefront shaping,” Optica (Preprint), Sep. 2021, doi: 10.1364/OPTICA.446178.